Hindawi
Shock and Vibration
Volume 2021, Article ID 8854538, 21 pages
https://doi.org/10.1155/2021/8854538

Research Article

Effect of Gas on Burst Proneness and Energy Dissipation of Loaded Coal: An Experimental Study Using a Novel Gas-Solid Coupling Loading Apparatus

Zuguang Wang[1,2] **Huamin Li**,[1,2] **Shen Wang**,[1,2,3] **Baobin Gao**[4] **and Wen Wang**[1,2]

[1]*School of Energy Science and Engineering, Henan Polytechnic University, Jiaozuo, Henan 454003, China*
[2]*State and Local Joint Engineering Laboratory for Gas Drainage & Ground Control of Deep Mines, Henan Polytechnic University, Jiaozuo, Henan 454003, China*
[3]*Postdoctoral Station of Safety Science and Engineering, Henan Polytechnic University, Jiaozuo, Henan 454003, China*
[4]*College of Safety Science and Engineering, Henan Polytechnic University, Jiaozuo, Henan 454003, China*

Correspondence should be addressed to Baobin Gao; gaobaobin@hpu.edu.cn

Received 13 July 2020; Revised 27 November 2020; Accepted 21 December 2020; Published 7 January 2021

Academic Editor: Jinjiang Wang

Deep coal mining is seriously affected by a combined dynamic disaster of rock burst and coal and gas outburst, but the influence mechanism of gas on this combined dynamic disaster is still not very clear, which is significantly different from the single type disasters. In this study, to explore the effect of gas on the coal-rock burst, a novel gas-solid coupling loading apparatus is designed to realize gas adsorption of coal sample with burst proneness and provide uniaxial loading environment under different gas pressure. A series of uniaxial compression tests of gas-containing coal with different gas pressure is carried out, and the energy dissipation process is monitored by an acoustic emission (AE) system. Results show that the macroscopic volume strain of the coal sample increases as gas adsorption and gas pressure increase under constant uniaxial loading pressure. Gas has the ability to expand the pores and natural fractures in coal sample by mechanical and physicochemical effects, which leads to a degradation in microstructure integrity of coal sample. With the increase of gas pressure, both the macrouniaxial compression strength (UCS) and elastic modulus show a downward trend; the UCS and elastic modulus of coal samples with 2 MPa gas pressure reduce by 58.78% and 48.82%, respectively, compared to those of the original coal samples. The main reason is that gas changes the pore-fissure structure and the mesoscopic stress environment inside the coal sample. Owing to the gas, the accumulated elastic energy of the gas-containing coal samples before failure reduces significantly, whereas the energy dissipated during loading increases, and the energy release process in the postpeak stage is smoother, indicating the participation of gas weakens the burst proneness of the coal sample. This study is of important scientific value for revealing the mechanism of combined dynamic disaster and the critical occurrence conditions of coal-rock burst and coal and gas outburst.

1. Introduction

With the gradual lack of shallow coal resources, the depth of coal mining increases rapidly in China. Under the deep mining conditions, the environment of coal mining working face emerges new characteristics, such as high in situ stress, high gas content, high temperature, and low permeability, which triggers more complex dynamic disasters [1–3]. It is well accepted that the coal and gas outburst and rock burst are the most serious dynamic disasters in coal mine, but they are usually studied separately due to the different mechanisms under the condition of shallow mining [1, 2]. Yuan pointed out that rock burst occurs mainly due to the sudden release of elastic potential energy stored in the coal and rock, while the main energy released during coal and gas outburst is the internal energy of gas in the coal [1]. With the increase of coal mining depth, the cause of dynamic disaster owing to the jointed effect of ground stress and gas is more and more significant, such as the '11.3' accident in Qianqiu coal mine in 2011, the '3.15' accident in Junde coal mine in 2013, and

the '12.22' accident in Gengcun coal mine in 2015 [4]. In the stage of deep mining, a new type of dynamic disaster in which coal and gas outburst and rock burst happen simultaneously is getting more and more attention. However, its occurrence mechanism is not clear, resulting in an open issue [5–8]. A large amount of elastic energy and gas internal energy can be accumulated in the coal-rock body affected by deep mining. At the same time, the original structure of coal mass is greatly changed by ground stress and gas pressure. The occurrence condition of combined dynamic disaster is lower than that of any single disaster, whereas the disaster intensity is increased [1]. Therefore, it is of practical significance to explore the failure characteristics of combined dynamic disaster by investigating the structure of coal-rock mass, gas pressure, and geo-stress.

In a coal mine, the coal pillar is widely used to maintain the stability of roadway and isolate longwall panel from gob, so its deformation and failure characteristics have a great impact on the stability of roof strata above longwall working face, and the subsidence of overlying strata also affects the internal structure of the coal pillar [9]. Limited by the mining technical conditions, isolated island or peninsula coal pillars are often left, as shown in Figure 1. The coal pillar is subjected to a vertical load in macroscopic view, which can be considered in the state of uniaxial compression [10]. Gob pillar experiences several mining stages: roadway driving and mining in the two side panels, resulting in crack propagation in coal pillars. The instability of coal pillars may bring burst into the coal seam and even cause dynamic disasters [9, 11–13]. From the above analysis, it can be found that the island-shaped coal pillar is in a state similar to uniaxial compression and is affected by the combined effect of high stress induced by roof structure and the residual gas in the gob. Therefore, the mechanism of the dynamic disaster of the coal pillar can be investigated by simplifying a model of gas-containing coal under uniaxial compression.

Coal is a composite material with multiple pores and fissures, especially affected by the mining activities such as roadway driving and longwall mining, providing channels and space for gas migration, diffusion, adsorption, and desorption [14, 15]. The gas in the coal pillar is mainly in the free state and adsorbed state. The free-state gas takes the form of pore pressure as the volume force to affect the mechanical property of coal, while the adsorbed gas affects the constitutive relation of the coal through adsorption and desorption [16–19]. During longwall mining, the gas in the coal pillar is in a dynamic change process of adsorption and desorption due to the variations of natural fractures, stress state, and gas migration in the coal pillar. L.D. Connell considers that sorption strain has a direct independent effect on permeability, pore pressure, and confining pressures [20]. He and Chen found that the expansion deformation of the coal sample occurs during the adsorption of CO_2 and CH_4 and is proportional to the increase of gas pressure [21, 22]. ZHAI studied the swelling deformation characteristics of coals with different particle sizes after gas absorption and found that the expansion deformation is different under different particle sizes [23].

According to the above, a large number of significant research studies have been carried out on the physical and mechanical characteristics, AE characteristics, and energy dissipation characteristics of gas-containing coal. These achievements play an important role in the study of the damage of gas-containing coal and the prevention and control of coal, rock, and gas combined dynamic disaster. However, at present, the research on the failure of gas-containing coal in the laboratory is mostly under triaxial or quasi-triaxial compression loading, and the research under uniaxial loading is lacking. The determination of the burst proneness of coal is mostly under uniaxial condition, so it is necessary to conduct in-depth study on the failure characteristics of gas-containing coal under uniaxial compression. In our study, a novel gas-solid coupling loading device is independently developed to conduct the uniaxial compression loading and unloading tests for coal samples under different gas pressures, during which the data of deformation, stress, and AE is monitored. The influence of gas on the physical and mechanical property, AE characteristics, and energy dissipation of coal samples, as well as the relationship among those parameters is analyzed. This study is of important scientific value for revealing the mechanism of combined dynamic disaster and the critical occurrence conditions of coal-rock burst and coal and gas outburst.

2. Materials and Methods

2.1. Coal Sample Preparation and Device Development

2.1.1. Collection and Preparation of Coal Samples. The coal samples with burst proneness were collected from the coal seam No. 22 in Bulianta coal mine located in Ordos, China. The coal seam No. 22 is concentrated in the Cretaceous, Jurassic Zhiluo Formation, and its basic physical and mechanical property is shown in Table 1.

To avoid the influence of coal heterogeneity and bedding fracture, the following points should be paid attention to ensure the original characteristics of coal samples as much as possible. (1) Select coal samples from the same working face. (2) Avoid collecting coal samples near fault and fold. (3) Minimize the damage to coal block caused by human activities during transportation. (4) Record in detail the collection time, location, type, and original property of coal samples.

The collected coal samples were processed into $\Phi 50\,\text{mm} \times 100\,\text{mm}$ samples according to the International Society for Rock Mechanics (ISRM) specifications. The accuracy of the processed coal sample must meet the following standards: (1) the nonparallelism of the two ends of the sample shall not be greater than 0.05 mm; (2) the diameter deviation of the upper and lower ends of the sample shall not be greater than 0.2 mm; (3) the surface of the sample must be smooth to avoid stress concentration during loading; (4) the axial deviation shall not be greater than 0.25°.

The prepared coal samples are divided into 6 groups for uniaxial compression and uniaxial loading-unloading tests with 0 MPa, 1 MPa, and 2 MPa gas pressure, respectively. To reduce the discreteness and contingency of the experiment,

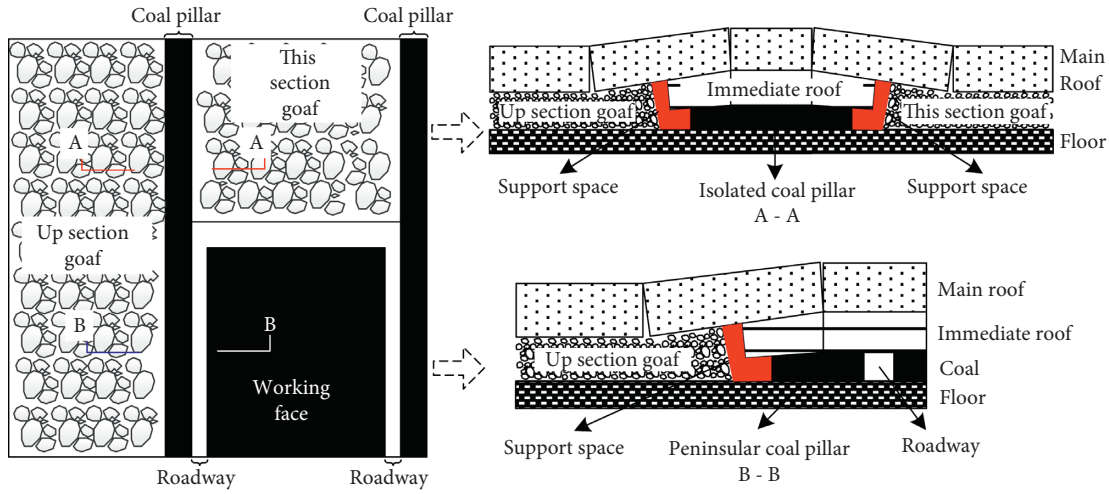

Figure 1: Diagrammatic drawing of isolated and peninsular coal pillar.

Table 1: Physical and mechanical parameters of coal seam No. 22 in Bulianta coal mine.

Parameters	Values
Wave velocity (m/s)	1266
Porosity (%)	9.9
Rock quality designation, RQD (%)	56.8
Cohesion (MPa)	19.3
Tensile strength (MPa)	1.2
Angle of internal friction (°)	24.5

at least 3 samples are prepared for each subtest, and the physical parameter values of the coal samples are shown in Table 2.

2.1.2. Test Device and System of Gas-Containing Coal under Uniaxial Compression

(1) The introduction of gas-solid coupling loading device: the development of the gas-solid coupling loading device was based on the idea of uniaxial compression experiment of gas-containing coal under zero effective confining pressure [24]. As shown in Figure 2, the new gas-solid coupling loading device mainly includes upper indenter, sealing cover, pressure chamber, base, and other parts. The pressure chamber is connected with the sealing cover and the base by bolts. A seal ring is arranged in the middle of the sealing cover, and a pressure regulating screw is arranged on the upper part of the combined seal ring to prevent gas leakage during the loading process. There is a groove under the center of the sealing cover, which is used to place the ultrasonic transducer (or alternative block), and the transducer is fixed on the lower part of the sealing cover by the retaining spring and the spring lid. The outer surface of the sealing cover is provided with an air outlet valve, and the inner part of the sealing cover is provided with an air vent for discharging air and gas. There is an air inlet valve in the middle of the pressure chamber for filling gas. A groove is arranged above the base to place the ultrasonic transducer (or alternative block), and a plurality of wire holes are uniformly arranged inside the base to install the strain gauge wire and the AE sensor wire, respectively. The strain gauge and the AE sensor are connected with the corresponding equipment outside through these wires to receive the strain and AE data. The coal sample is placed in a sealed container and filled with a certain pressure of high-purity gas; when the adsorption-desorption equilibrium state is reached, the free-state gas pressure in the coal body is applied to the coal skeleton, which equals the external gas pressure; then, the uniaxial loading can be applied.

The air tightness of the device was tested under static and dynamic air inflation, respectively. For the static air tightness test, first, gas of 0.5 MPa is inflated into the device; then, soapy water is smeared onto the joints, thread holes, and pressure rod pistons where gas leakage may occur. If bubbles are generated, it indicates that the sealing performance is poor at that place. For dynamic air tightness test, after inflating 0.5 MPa gas into the device and soapy water is smeared, the upper indenter is push down to apply compression force, during which the tightness is observed by the same approach of the static test.

(2) Development process of the gas-solid coupling loading device: the development process of this device, as shown in Figure 3, includes device design, part processing, line layout, air tightness test, sensitivity, and resistance calibration.

The device was installed on a mechanical loading machine and filled of 1 MPa and 2 MPa pressure gas to measure the sensitivity of collected signal and the friction resistance which makes the measured stress larger. Therefore, the friction resistance should be subtracted to obtain the real gas pressure. The resistance measurement curve under 1 MPa and 2 MPa gas pressure is shown in Figure 4, from which it can be found that the friction resistance under 1 MPa and 2 MPa gas pressures are 0.185 MPa and 0.236 MPa, respectively.

Table 2: Record of coal sample grouping and physical properties of coal samples.

Number	Diameter (mm)	Height (mm)	Density (kg•m^{-3})	Gas pressure (MPa)	Loading mode
B1-1	49.6	95.1	1271.9	0	Uniaxial compression
B1-2	49.5	99.3	1151.7		
B1-3	49.3	96.3	1212.1		
B1-4	49.7	97.3	1253.5		Uniaxial loading-unloading
B1-5	48.5	99.0	1287.4		
B1-6	49.5	98.8	1232.7		
B2-1	49.4	97.5	1330.2	1	Uniaxial compression
B2-2	49.5	99.2	1274.3		
B2-3	49.3	97.4	1376.7		
B2-4	49.4	98.3	1318.5		Uniaxial loading-unloading
B2-5	49.3	100.02	1238.0		
B2-6	50.0	99.3	1201.1		
B3-1	49.6	100.0	1292.4	2	Uniaxial compression
B3-2	49.5	98.1	1227.5		
B3-3	49.5	99.1	1344.4		
B3-4	49.5	99.2	1342.9		Uniaxial loading-unloading
B3-5	49.3	97.4	1376.7		
B3-6	49.5	95.8	1250.4		

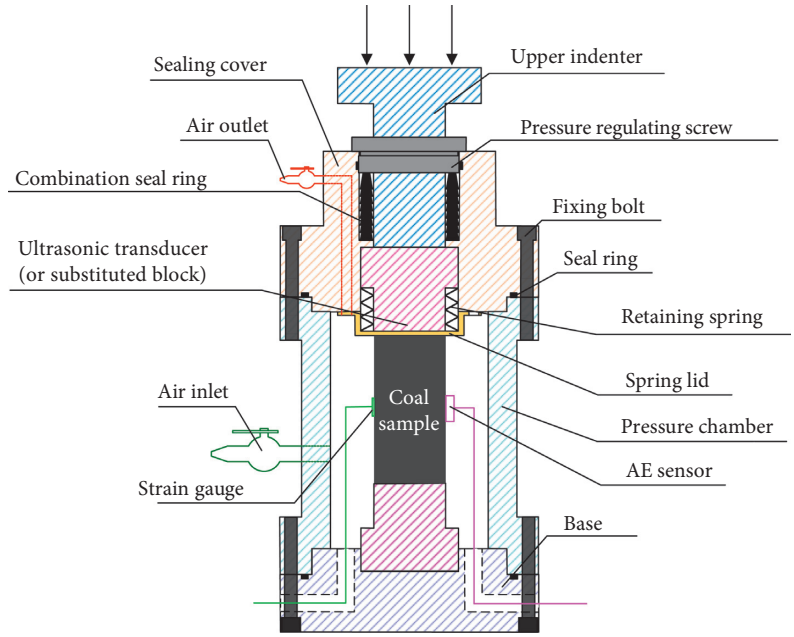

Figure 2: Schematic of the new gas-solid coupling loading device used in this study.

2.2. Experimental System and Testing Process. As shown in Figure 5, the gas-containing coal uniaxial compression test system consists of the gas-solid two-phase coupling loading device, electro-hydraulic servo controlled loading system, AE signal detection system, stress-strain monitoring and recording system, and vacuum pump and gas supply system.

2.2.1. Experimental System

(1) Loading system: an RMT-150C electro-hydraulic servo controlled rock mechanics testing machine was used to load the coal sample. The maximum axial force of the testing machine can reach 1000 kN, the displacement loading rate is 0.0001–1 mm/s, and the vertical piston stroke is 50 mm. The testing machine is equipped with force, stroke, vertical, and lateral displacement sensors, which can record stress, vertical, and lateral deformation in the loading process.

(2) AE monitoring system: a DS5 AE signal analyzer was used to collect the AE signal, of which the wave data passing rate is 192 MB/s, and the maximum sampling speed can reach 10 MHz. The acoustic emission sensors were closely attached onto both sides of the middle of the coal sample, and the coupling agents were applied between sensors and coal sample to reduce the gap between them. In this study, the AE monitoring threshold was set to 50 dB, the sampling

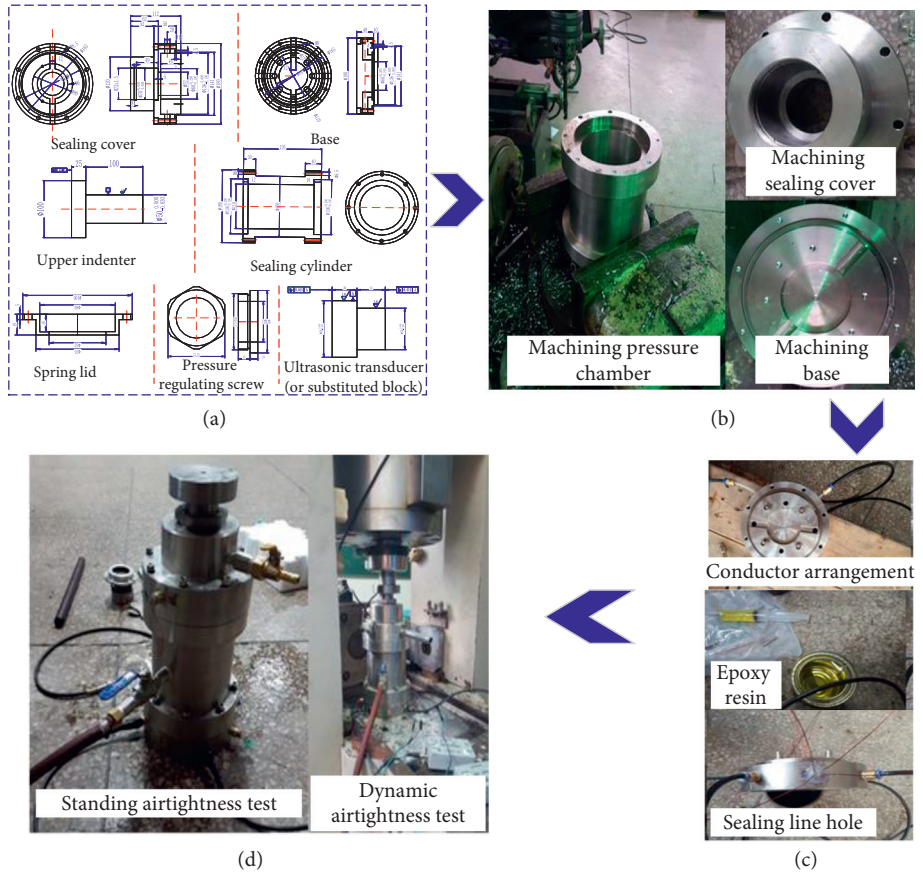

FIGURE 3: Schematic of the development process of the new gas-solid coupling loading device. (a) Device design. (b) Part processing. (c) Air tightness test. (d) Line layout.

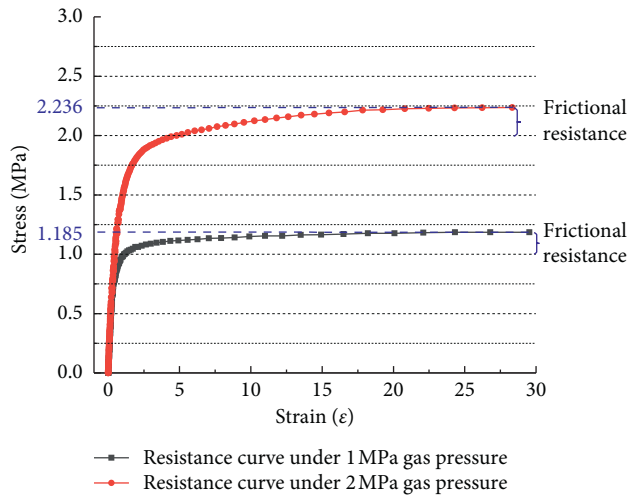

FIGURE 4: Testing curves of resistance.

frequency was set to 1 Msps, and the sampling rate was set to 1 kHz–3 kHz.

(3) Strain monitoring system: the XL2101 C program-controlled static resistance strain gauge was used to monitor the lateral and axial strains of coal samples in real time. The sampling frequency of the resistance strain gauge was 2 Hz, the resolution was 1 $\mu\varepsilon$, the measurement range was -19999 $\mu\varepsilon$ ~ + 38000 $\mu\varepsilon$, and the accuracy was ±0.2% ± 2 $\mu\varepsilon$. The bridge formation mode was mixed bridge formation and the two strain gauges were arranged vertically in the middle of the coal sample, and the computer monitoring mode was adopted.

(4) Gas supply system: the air supply system was composed of a high-pressure gas cylinder, vacuum

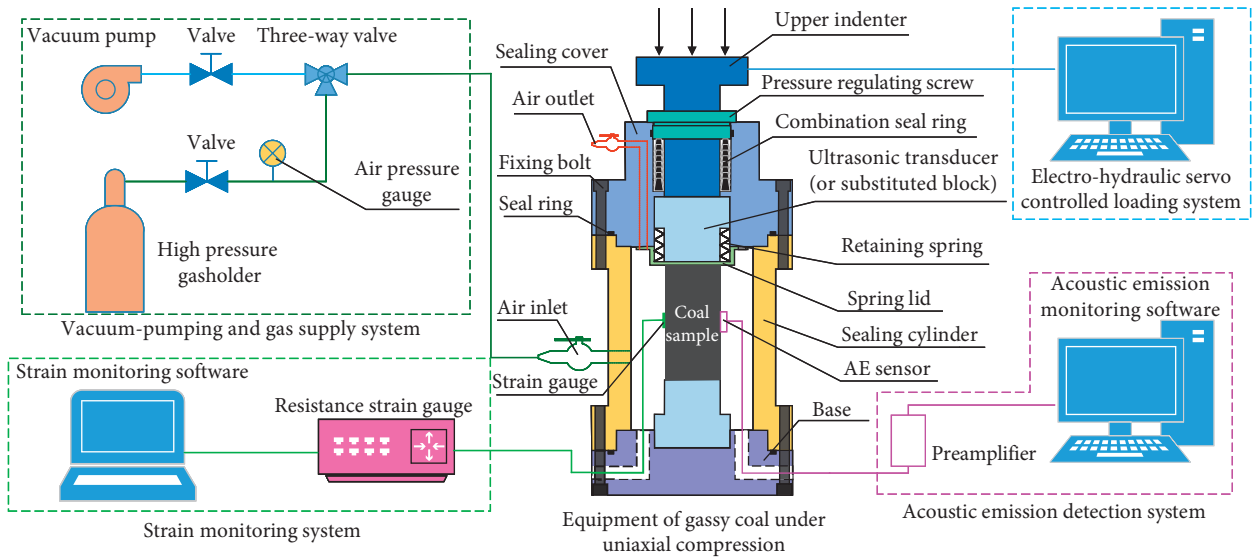

Figure 5: Schematic of the experiment system for the gas-containing coal under uniaxial compression test.

pump, pressure gauge, pressure-reducing valve, and high-pressure pipe. The maximum pressure of high-pressure gas cylinder is 5 MPa, and the maximum vacuum degree of the vacuum pump is −0.1 MPa. After the device was installed and placed on the loading test machine, the vacuum pump was connected with the air outlet of the device, and then the air outlet valve was opened for air extraction and the air outlet valve was closed after vacuuming. The main valve of the high-pressure gas cylinder was externally connected to a pressure reducing valve, which was connected to the air inlet on the pressure chamber through the high-pressure pipe. The gas pressure in the experimental device was controlled by adjusting the gas cylinder master valve and the pressure reducing valve so that the coal sample was in an environment where the gas pressure was set.

2.2.2. Experimental Steps. The test method was based on Chinese standard for the determination of the burst tendency of coal-rock samples "Methods of Determination, Monitoring, and Prevention of Rock Burst, Part 2: Classification Method and Index of Burst Tendency of Coal" (GB/T 25217.2–2010).

(1) Coal samples were grouped according to gas pressure and loading mode as multifactor tests. A total of 6 groups of tests were performed, which are shown in Table 2.

(2) Conventional uniaxial compression experiment: the coal samples attached with the AE sensors were placed on the base of the rock mechanics testing machine. The AE sensors were connected to the AE monitor and the tip of the lateral displacement sensor were adhered lightly against the surface of the coal wall. According to the burst tendency index test method, the uniaxial compression test and uniaxial loading-unloading test were carried out, and the physical and mechanical parameters, deformation parameters, and AE parameters of the coal samples were recorded.

Gas-containing coal uniaxial compression test: the coal samples attached with the AE sensors and strain gauge were placed in the center of the base of gas-solid two-phase coupling loading device, and then the pressure chamber and the sealing cover were installed orderly. The base, the sealing cover, and the pressure chamber were fixed with bolts. The assembled device was placed directly under the indenter of RMT-150C rock mechanics testing machine, and the wires installed on the base of the device were connected with the AE monitor and the strain monitor, respectively. After the installation of the device, the air tightness of the device must be checked. A certain pressure gas shall be introduced into the test device, and a layer of soapy water shall be coated at each interface of the device. If the air tightness of the device is good, the test can be carried out; otherwise, the air tightness of the device shall be improved to good before the test. Then, the vacuum pump was connected to the air outlet of the device for vacuumizing. When the vacuum degree reached −0.1 MPa, the air outlet valve was closed and the vacuum pump was removed. The high-pressure gas cylinder was connected to the air inlet of the device, and the main valve, pressure reducing valve, and air inlet valve of the device to inflate were opened to inflate so that the coal sample in the pressure chamber was under the set gas pressure (1 MPa or 2 MPa) until the adsorption was saturated (the basis for determining adsorption saturation is that the readings of pressure gauge and strain gauge will not change any more, that is, the gas pressure inside the pressure chamber and the axial and lateral deformation of the coal sample will not change). Then, the main valve, pressure-reducing valve, and unit intake valve were closed in turn. According to the burst tendency index test method, the uniaxial

compression test and uniaxial loading-unloading test were carried out, and the physical and mechanical parameters, deformation parameters, and AE parameters of the coal samples were recorded.

3. Experimental Results

3.1. Volume Change of Coal Sample during Gas Filling and Adsorption. The resistance strain gauge was used to monitor the lateral and axial strain of the coal sample in the process of gas filling and gas absorption, so as to reflect the influence of gas on the volume of the coal sample.

(1) Gas filling progress: the gas filling process of the test was that the pressure reducing valve was opened several times and the gas slowly filled the device until it reached the set gas pressure. A Xl2101 C program-controlled static resistance strain gauge was used to collect the lateral and axial strains of the coal samples during the filling process. See Table 1, for the strain of the coal samples during this process which can be seen in Table 3. The gas filling pressure is positively correlated with the lateral and axial strain of the coal sample. The average axial and lateral strains of the coal sample are 1364 $\mu\varepsilon$ and 817 $\mu\varepsilon$, respectively, when gas filling pressure is 1 MPa. The average axial and lateral strains of the coal sample are 1946 $\mu\varepsilon$ and 1001 $\mu\varepsilon$, respectively, when gas filling pressure is 2 MPa, and the axial strain increased by 42.6% and the lateral strain increased by 22.5% compared with filling 1 MPa gas pressure to coal samples. The results show that the larger the filling gas pressure is, the greater the influence on the deformation of coal sample is.

(2) Gas adsorption process: the gas adsorption process started from the end of filling gas and continued until the gas adsorption saturation of the coal sample, that is, the axial and lateral strain of the coal sample did not change greatly. After the gas filling process was completed and the deformation data was recorded, the dial reading was reset to 0. The XL2101 C program-controlled static resistance strain gauge was used to collect the axial and lateral strains of the coal samples during the gas adsorption process. The strain of coal sample during adsorption is shown in Table 4 and Figure 6.

As shown in Table 4, the average axial strain is 1512 $\mu\varepsilon$ and the lateral strain is 1227 $\mu\varepsilon$ after adsorption saturation of coal sample under 1 MPa gas pressure. The average axial strain and lateral strain are 2598 $\mu\varepsilon$ and 1907 $\mu\varepsilon$, respectively, after adsorption saturation of the coal sample under 2 MPa gas pressure, and the axial strain and lateral strain increase by 71.8% and 55.4%, respectively, compared with the 1 MPa gas pressure condition. The results show that there is a positive correlation between the gas pressure and the deformation amount of the coal sample after adsorption saturation. Figure 6 shows that there are two stages, rapid deformation stage and slow deformation stage, of the change trend of the axial and lateral strain in the process of coal sample adsorption under different gas pressures. It can be seen from Figure 6 that the variation trend of the deformation curve after peak deformation is relatively gentle, so we judge that the cut-off point of these two stages is before the peak deformation. According to the deformation data collected, the growth rate of the deformation curve before the peak deformation was calculated. When the growth rate was less than 1%, we believed that the curve's change trend was relatively slow, that is, it was in the slow deformation stage, and the previous stage was divided into the rapid deformation stage.

3.2. Mechanical Properties of Coal Samples. Figure 7 shows relationship between UCS, elastic modulus, and gas pressure, and Table 5 is the statistical table of mechanical parameters of gas-containing coal samples in the uniaxial compression test.

From Figure 7 and Table 5, it can be seen that, with the increase of gas pressure from 0 MPa to 2 MPa, the average UCS of coal sample decreases from 31.66 MPa to 13.05 MPa, decreasing by 58.78%; the average elastic modulus of the coal sample decreases from 2.11 GPa to 1.08 GPa, decreasing by 48.82%; the average Poisson's ratio of coal sample increases from 0.29 to 0.40, increasing by 37.93%. Generally speaking, with the increase of gas pressure in the coal samples, the UCS and elastic modulus of the coal samples are decreased, and Poisson's ratio of the coal sample is increased.

3.3. Elastic Strain Energy Index. The Elastic Strain Energy Index (W_{ET}) reflects the storage capacity of the elastic properties in the of coal skeleton during uniaxial compression. In the process of external loading, some of the coal samples have plastic deformation and energy dissipation and some of them have elastic deformation and energy accumulation. After unloading, the deformation caused by elastic energy can be recovered, but the deformation is unable to restore after energy dissipation.

In the laboratory, the coal samples were uniaxially compressed in the form of forced loading (loading rate was 0.2 kN/s), which were loaded to 75%~85% of the average UCS and then unloaded to 0 kN at the same rate to obtain the uniaxial loading-unloading curve of the coal sample. The ratio of elastic deformation energy to plastic deformation energy is taken as the elastic strain energy index of the coal sample, as shown in Figure 8, and the calculation formulas are shown in equations (1) to (4) [25]:where W_{SE} is the elastic strain energy, which represents the accumulated elastic strain energy during loading, kJ/m^3; W_C is the total strain energy, which represents the total work done by external loads during the loading process, kJ/m^3; W_{SP} is the plastic strain energy dissipated during loading, kJ/m^3; σ_L and σ_{UL} are the stress values under the loading and unloading path of coal samples, respectively, MPa; ε_1 and ε_2 denote the corresponding strain value when unloading completely and at unloading point. The loading and unloading curves of coal samples under different gas pressures are shown in Figure 9.

Table 3: Statistics of axial and lateral strain of the coal sample in the aeration process.

Sample ID	Gas pressure/MPa	Axial strain ($\mu\varepsilon$)		Lateral strain ($\mu\varepsilon$)	
		Test value	Average value	Test value	Average value
B2-1		1960		1514	
B2-2	1	1002	1364	633	817
B2-3		1130		305	
B3-1		2055		1508	
B3-2	2	1777	1946	554	1001
B3-3		2006		942	

Note. 1 $\mu\varepsilon$ is one millionth.

Table 4: The statistics of axial and lateral strain of the coal sample in the adsorption process.

Sample ID	Gas pressure (MPa)	Axial strain ($\mu\varepsilon$)		Lateral strain ($\mu\varepsilon$)	
		Test value	Average value	Test value	Average value
B2-1		1845		1606	
B2-2	1	1687	1512	1296	1227
B2-3		1004		779	
B3-1		2497		2053	
B3-2	2	2435	2598	2487	1907
B3-3		2863		1183	

Note. 1 $\mu\varepsilon$ is one millionth.

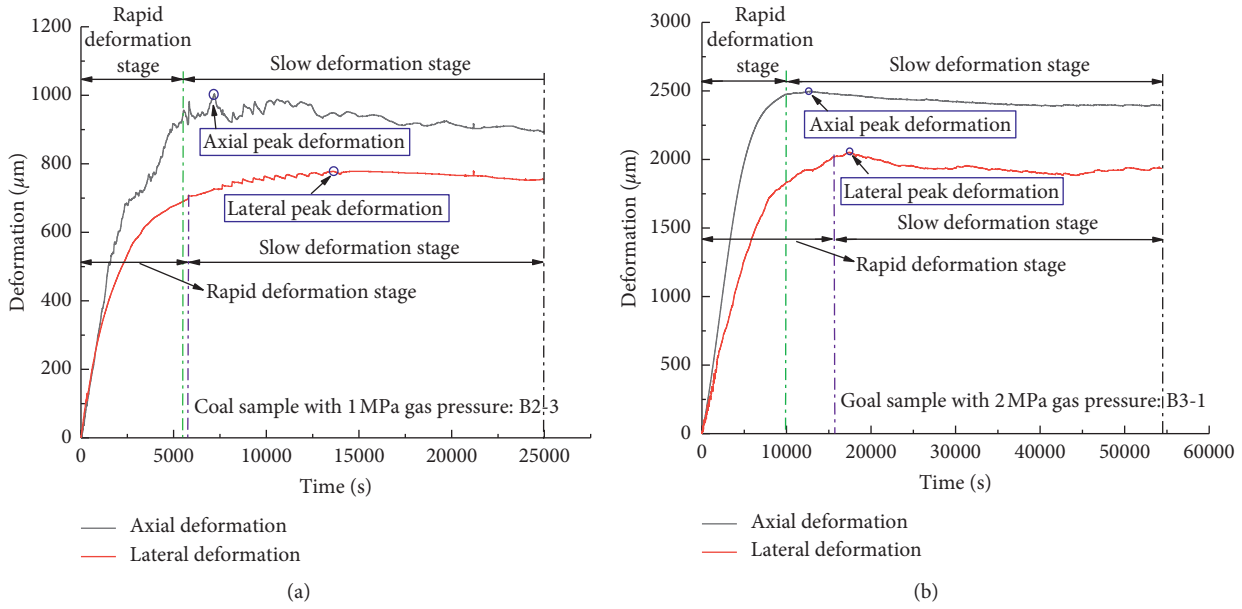

Figure 6: The deformation figure of the coal sample in the stable process. (a) Coal sample with 1 MPa gas pressure. (b) Coal sample with 2 MPa gas pressure.

$$W_{ET} = \frac{W_{SE}}{W_{SP}}, \tag{1}$$

$$W_C = \int_0^{\varepsilon_2} \sigma_L \mathrm{d}\varepsilon, \tag{2}$$

$$W_{SE} = \int_{\varepsilon_1}^{\varepsilon_2} \sigma_{UL} \mathrm{d}\varepsilon, \tag{3}$$

$$W_{SP} = W_C - W_{SE}, \tag{4}$$

Figure 10 shows the relationship between W_{ET} and gas pressure, and Figure 11 shows the ratio of elastic strain energy and plastic strain energy to total energy in the loading process of gas-containing coal samples. It can be obtained that, with the increase of gas pressure in the coal sample from 0 MPa to 2 MPa, the elastic strain energy index of the coal sample shows a decreasing trend. The W_{ET} of the coal sample decreases from 8.09 to 1.08, which decreases by 86.65%. The ratio of elastic strain energy decreased from 0.89 to 0.52, and the ratio of dissipated energy increased from

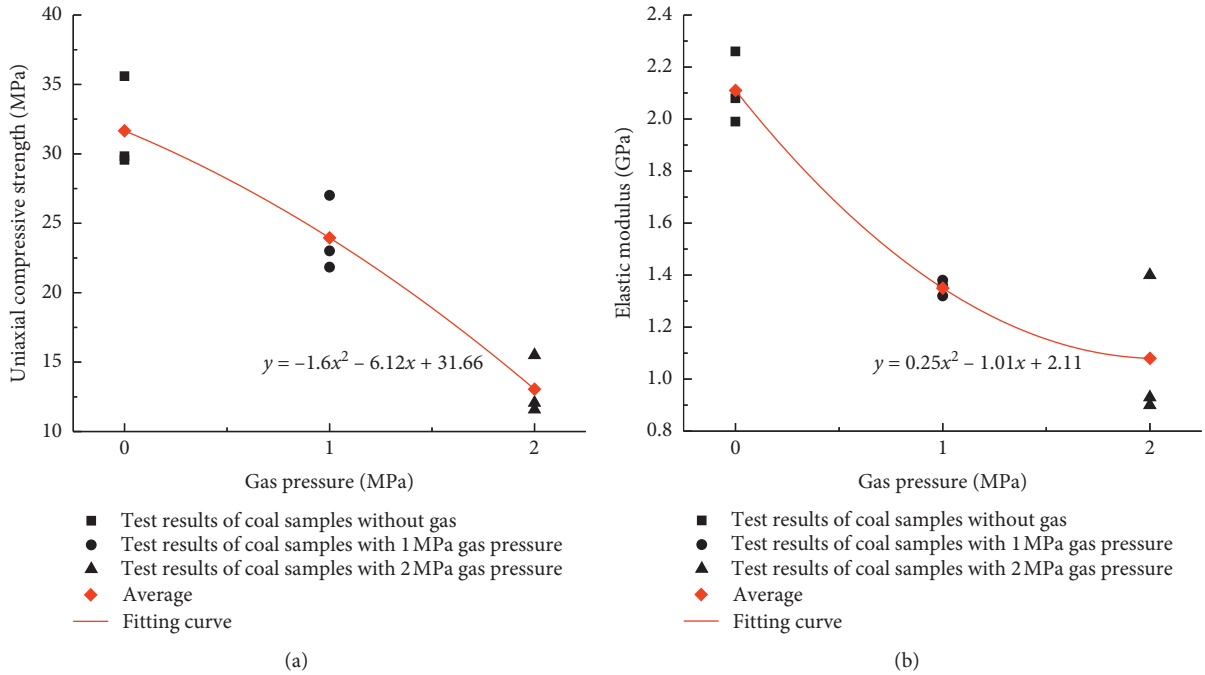

Figure 7: Relationship between UCS, elastic modulus, and gas pressure.

Table 5: Results of the mechanical property of coal samples under different gas pressures.

Gas pressure (MPa)	Sample ID	σ_C (MPa)		E (GPa)		ν	
		Test value	Average value	Test value	Average value	Test value	Average value
0	B1-1	29.83	31.66	2.08	2.11	0.28	0.29
	B1-2	35.59		2.26		0.30	
	B1-3	29.56		1.99		0.29	
1	B2-1	21.84	23.95	1.32	1.35	0.32	0.31
	B2-2	27.01		1.36		0.23	
	B2-3	23.01		1.38		0.38	
2	B3-1	12.07	13.05	1.40	1.08	0.33	0.40
	B3-2	11.59		0.93		0.48	
	B3-3	15.50		0.90		0.39	

Note. σ_C = UCS; E = elastic modulus; ν = Poisson's ratio.

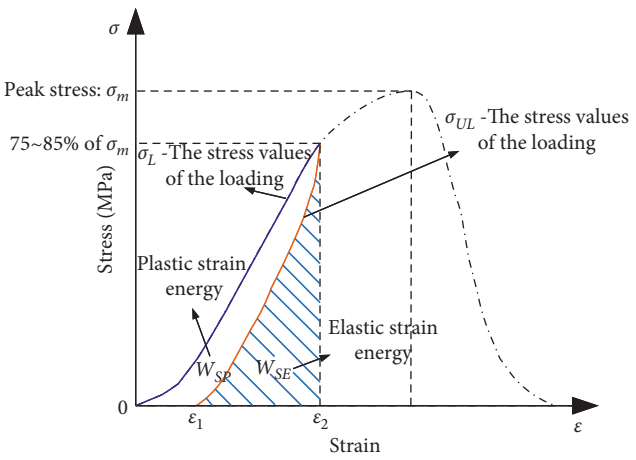

Figure 8: Schematic of elastic strain energy index calculation.

0.11 to 0.48, which shows that the proportion of elastic deformation decreases and the proportion of plastic deformation increases when the coal sample is loaded externally.

Figure 12 shows the energy change curve of loading and unloading of gas-containing coal samples. With the increase of gas pressure, the horizontal distance from the end of unloading curve to the origin becomes larger, that is, the larger the ratio of residual deformation to total deformation. The average ratio of residual deformation is 9.3% for coal samples without gas, whereas 29.4% and 44.1%, respectively, with 1 MPa and 2 MPa gas pressures. Meanwhile, with the increase of gas pressure, the vertical distance between the energy value corresponding to the end of unloading curve and the origin becomes larger, which means that the ratio of plastic strain energy to total work carried out by external load to the coal sample is larger.

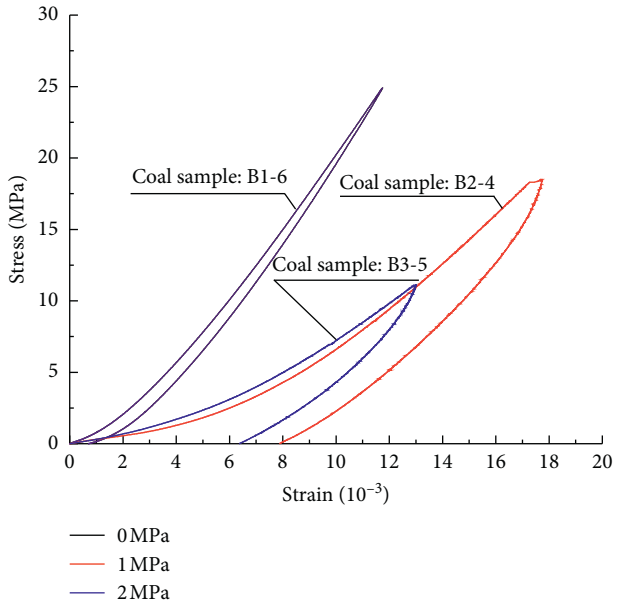

Figure 9: Loading and unloading curves of coal samples.

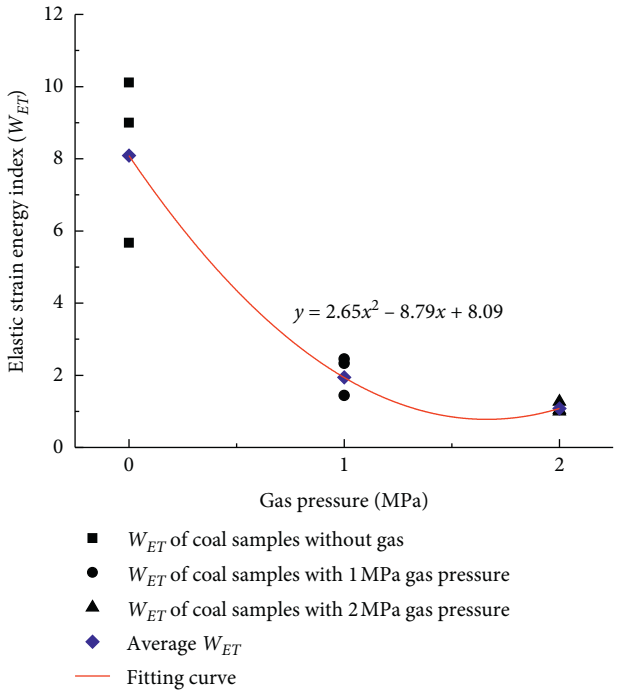

Figure 10: Relation curve between W_{ET} and gas pressure.

3.4. Impact Energy Index. The Impact Energy Index (K_E) reflects the degree of energy dissipation in the process of coal loading to failure. The more the energy dissipation, the smaller the residual energy of the coal sample and the smaller the energy converted into kinetic energy, thermal energy, and radiation energy when the coal sample is damaged, otherwise, the larger. K_E is the ratio of the deformation energy accumulated before the peak to the deformation energy dissipation after the peak in the stress-strain curve of the coal sample under uniaxial compression, as shown in Figure 13. The calculation formulas are shown in equations (5)–(7) [25]:where W_S is the prepeak stress accumulated deformation energy, kJ/m^3; W_E is the postpeak dissipated deformation energy, kJ/m^3; σ_L is the stress value under the loading path of coal samples, MPa; ε_3 and ε_4 are severally the strain value corresponding to peak stress and failure of the coal sample.

$$K_E = \frac{W_S}{W_E}, \tag{5}$$

$$W_S = \int_0^{\varepsilon_3} \sigma_L \mathrm{d}\varepsilon, \tag{6}$$

$$W_E = \int_{\varepsilon_3}^{\varepsilon_4} \sigma_L \mathrm{d}\varepsilon, \tag{7}$$

Figure 14 shows the relationship between K_E and gas pressure, and Figure 15 is a histogram of the percentage of prepeak and postpeak energy in the total energy of gas-containing coal during loading. It can be seen that, with the increase of gas pressure, the average postpeak dissipated deformation energy increases from 8% to 23% of the total energy, but the increase range of dissipated energy decreases. The proportion of dissipative energy increases by 112.5% from the coal sample without gas to the gas pressure containing 1 MPa, and the proportion of dissipative energy increases only by 35.3% from the coal sample with 1 MPa gas pressure to the gas pressure containing 2 MPa. At the same time, the average K_E of the coal sample decreases from 39.18 to 3.97, which decreased by 89.87%. Therefore, the gas has a significant influence on the increase of postpeak dissipation energy which is more obvious when there is gas or not, and the increase trend of postpeak dissipation energy is slowed down between gas-containing coal samples.

3.5. AE Characteristics

(1) AE count characteristics: Table 6 shows the AE count and cumulative count record of uniaxial compression process under different gas pressure conditions, and Figure 16 shows the relationship between acoustic emission signal and stress-strain curve of uniaxial compression failure process under different gas pressure conditions.

According to Figure 16 and Table 7, the AE peak energy and AE cumulative energy in the process of coal failure are negatively correlated with the gas pressure of the coal sample. The average AE peak energy in the coal sample with 0 MPa, 1 MPa, and 2 MPa gas pressures is 6292.6 mV·ms, 2950.7 mV·ms, and 2151.8 mV·ms, respectively, and the average AE cumulative energy is 458662.8 mV·ms, 393460.7 mV·ms, and 275986.2 mV·ms, respectively. With the increase of gas pressure from 0 MPa to 2 MPa, the average AE peak energy of acoustic emission is reduced by 65.8%, and the average AE cumulative energy of acoustic emission is reduced by 41.7%, which shows that the proportion of strain energy generated by brittle fracture of the

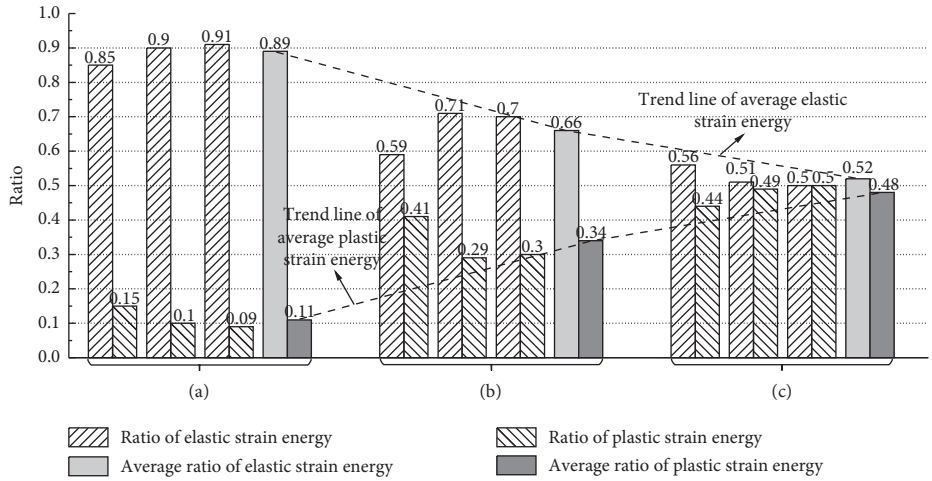

Figure 11: Ratio of elastic energy and dissipation energy during loading and unloading. (a) Coal samples without gas. (b) Coal samples with 1 MPa gas pressure. (c) Coal samples with 2 MPa gas pressure.

gas-containing coal sample is lower than that of gas-free coal sample.

The change rule of AE energy parameters in the process of coal loading reflects the law of its fracture development. Under the condition of external loading, the coal experiences a process of "compression closure, crack generation, development, and coalescence," and the change of cracks is accompanied by the generation of AE energy. Correspondingly, the energy of AE emission corresponded to the initial quiescence period, AE active period, and late quiescence stage. The participation of gas increases the number of initial cracks in the coal sample, so there are more cracks closed in the compaction stage of gas-containing coal and will be more AE events. In the elastic deformation and plastic deformation stage, the original coal samples need more energy to generate new fractures and promote the expansion of new fractures. Gas-containing coal is conducive to the development of fractures in the process of loading due to gas's destructive effect on the skeleton of coal samples. Compared with the coal samples without gas, the energy required to generate fractures is relatively less. Therefore, compared with the coal samples without gas, the AE energy in the active period of gas-containing coal is relatively smaller in the peak value, total amount, and proportion of energy in the whole loading process. In the postpeak failure stage, the coal samples without gas have the characteristics of brittle failure, and the failure process is transitory and violent. The ductile failure characteristics of the gas-containing coal samples are relatively obvious, and the failure duration is long.

It can be seen from Table 6 and Figure 16 that there is a good correspondence between the AE count and the stress-strain curve of the coal sample during the uniaxial compression of the gas-containing coal sample, and the peak value of the AE count appears near the large fracture of the coal sample (as shown in Figures 15(a)–15(c)). The average AE peak counts of 0 MPa, 1 MPa, and 2 MPa are 2080, 1704, and 1407, respectively, and the average AE cumulative counts are 348617, 295627, and 208707, respectively. With the increase of gas pressure from 0 MPa to 2 MPa in the coal sample, the average AE peak counts decrease by 32.4% and the average AE cumulative counts decrease by 40.1%. That is to say, there is a negative correlation between the AE peak count and cumulative count and the gas pressure of the coal sample.

It can be seen from Figure 16 that the development process of coal sample failure is different from the AE cumulative counting curve. The AE cumulative counting curve of coal samples without gas is similar to a straight line, while the AE cumulative curve of gas-containing coal samples has less AE events in the compaction stage, and the generation rate of AE events in the elastic deformation and plastic deformation stage has a significant increase, and the AE events in the postpeak deformation stage show a nearly vertical upward trend. The initial fracture of the brittle coal sample is less without gas. From the beginning of loading, there are a lot of cracks forming, developing, and expanding, which quickly lose bearing capacity after reaching the peak stress. However, the initial fracture of gas-containing coal increases, and the AE events in the compaction stage of loading is mostly the closure of fracture, with small intensity. In the plastic deformation stage, a large number of new fractures develops and grows from the pre-existed micronatural fractures. In the destruction process of coal samples, the average AE events in the compaction and elastic stages account for a small proportion of the total AE events; those of coal samples without gas, with 1 MPa gas pressure and 2 MPa gas pressure, are 8%, 19%, and 14%, respectively. However, the average AE events in the plastic deformation stage take up a significant proportion, which are 91%, 74%, and 84%, under the conditions of no gas, 1 MPa gas pressure and 2 MPa gas pressure, respectively. As the ductility of the coal sample enhances, the coal sample still has a certain bearing capacity after reaching the peak stress, and

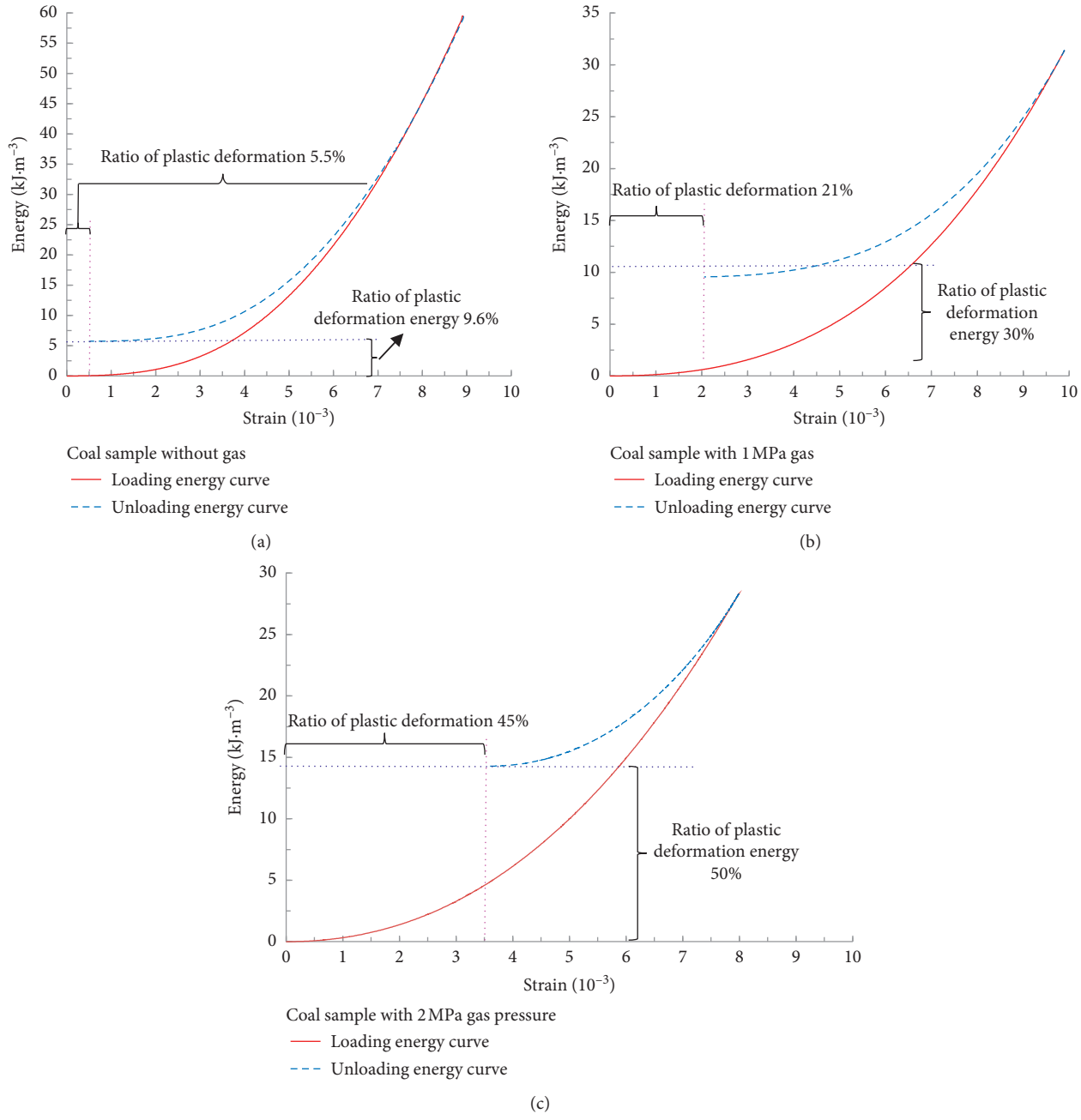

Figure 12: Energy evolution curve of gassy coal during loading and unloading. (a) Coal sample without gas pressure. (b) Coal sample with 1 MPa gas pressure. (c) Coal sample with 2 MPa gas pressure.

the sliding and friction between the coal blocks can still produce AE events.

(2) AE energy characteristics: Table 7 is the recording table of AE energy signal under uniaxial compression for different gas pressure coal samples, and Figure 15 is the relationship curve of AE energy and AE cumulative energy with stress and time under uniaxial compression for different gas pressure coal samples.

3.6. Energy Dissipation Characteristics. The failure of coal and rock under load is a process of energy accumulation and dissipation in materials, which constantly exchanges material and energy with the external environment. Under the loading condition in laboratory, the mechanical energy exerted by the testing machine is partly transformed into the releasable elastic energy stored in the coal body and partly transformed into the dissipative energy. No heat exchange

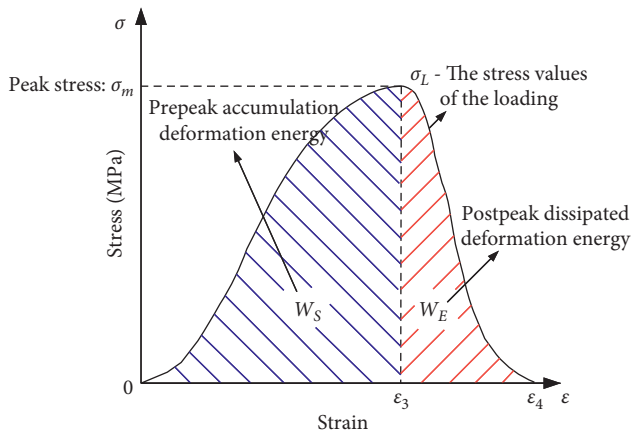

Figure 13: Legend of Impact Energy Index calculation.

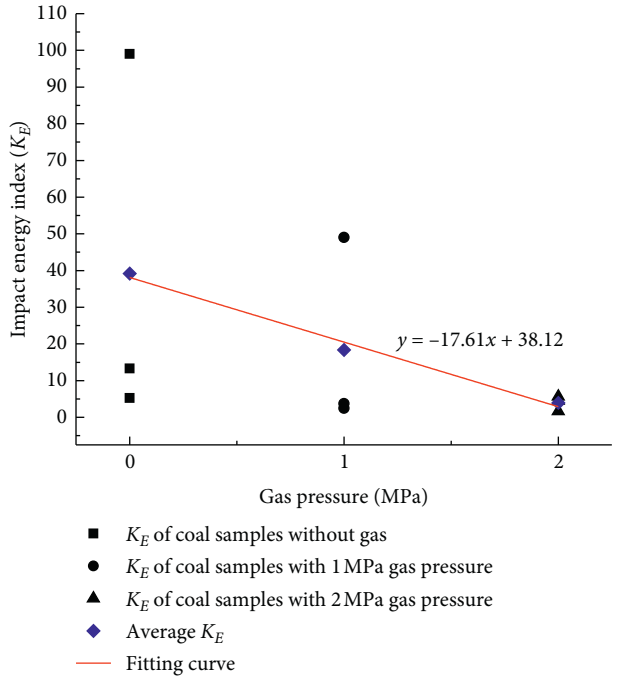

Figure 14: Relation curve between K_E and gas pressure.

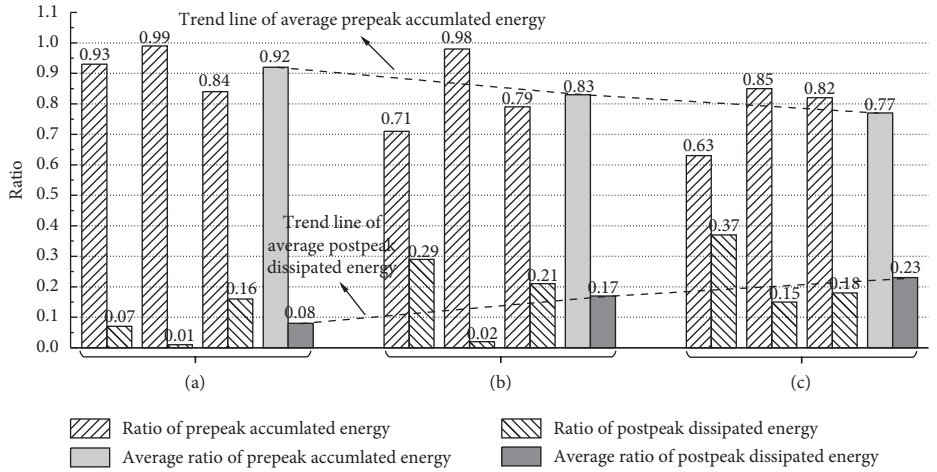

Figure 15: Ratio of prepeak energy and postpeak energy of gas-containing coal. (a) Coal samples without gas. (b) Coal samples with 1 MPa gas pressure. (c) Coal samples with 2 MPa gas pressure.

Table 6: AE signal of coal samples with different gas pressures under uniaxial loading.

Sample ID	Gas pressure (MPa)	Peak counts (times)		Cumulative counts (times)	
		Test value	Average value	Test value	Average value
B1-1	0	2116	2080	363079	348617
B1-2		1948		343265	
B1-3		2178		339508	
B2-1	1	1580	1704	278385	295627
B2-2		1624		298176	
B2-3		1910		310320	
B3-1	2	1373	1407	172434	208707
B3-2		1537		217808	
B3-3		1312		234777	

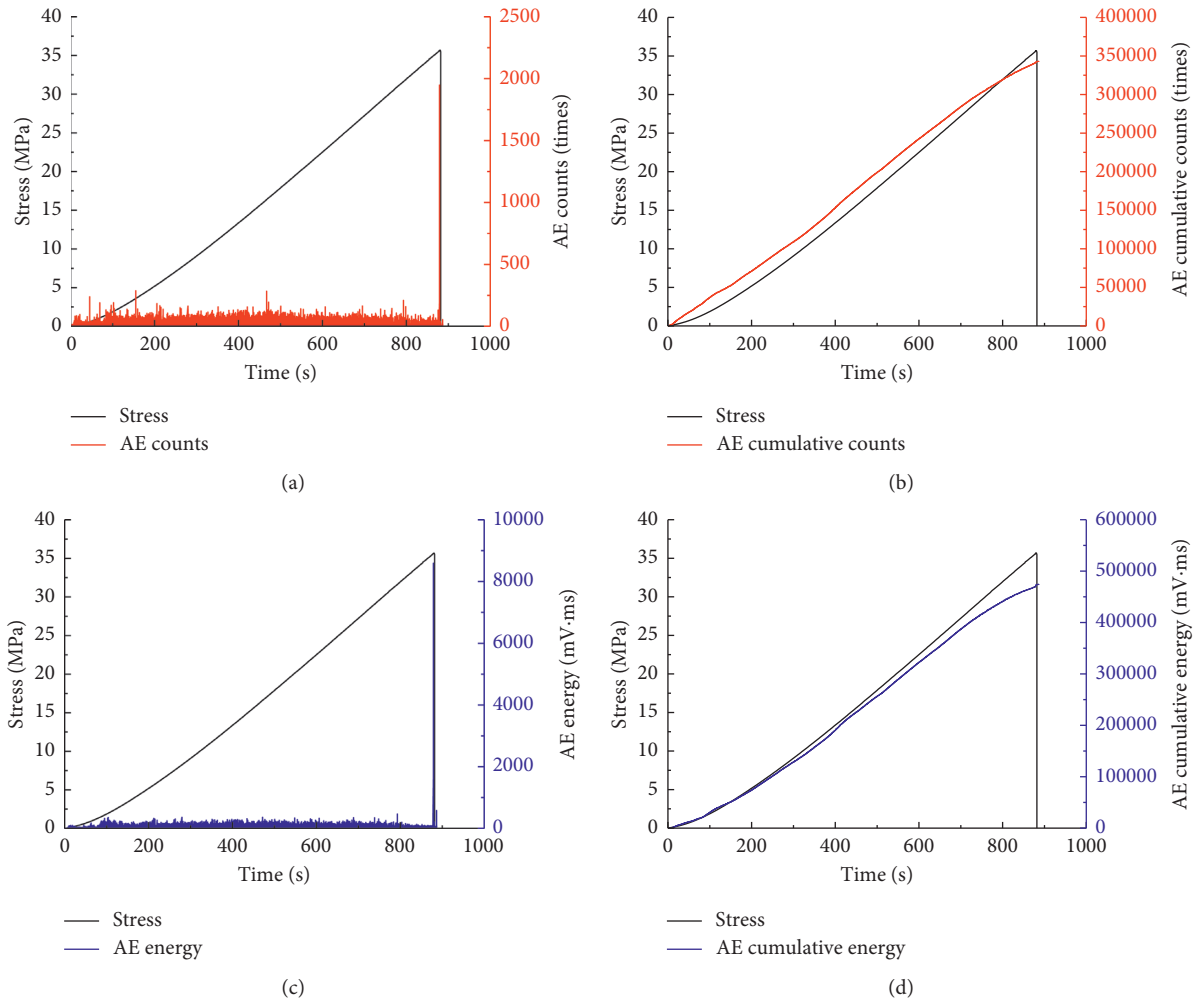

Figure 16: Continued.

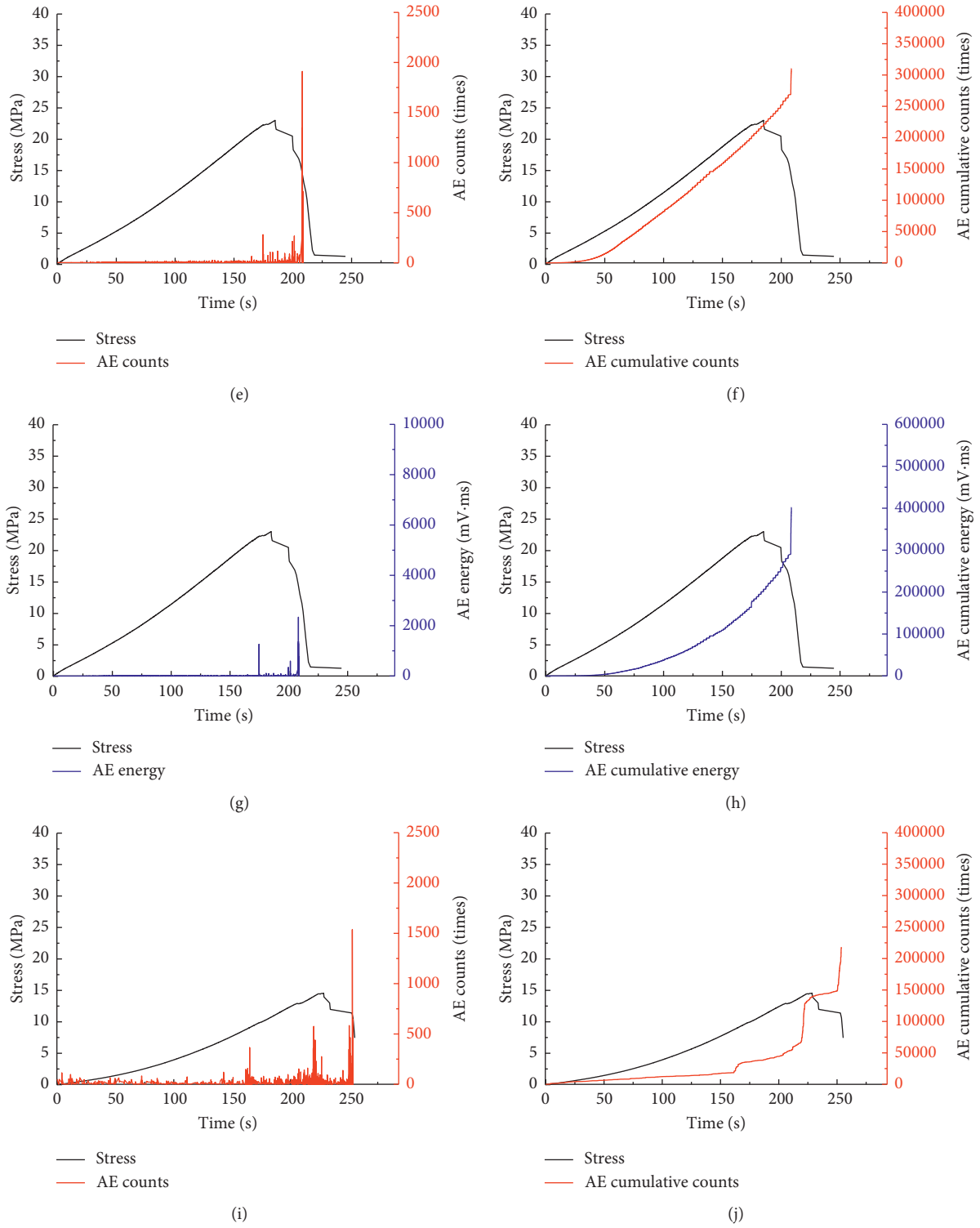

Figure 16: Continued.

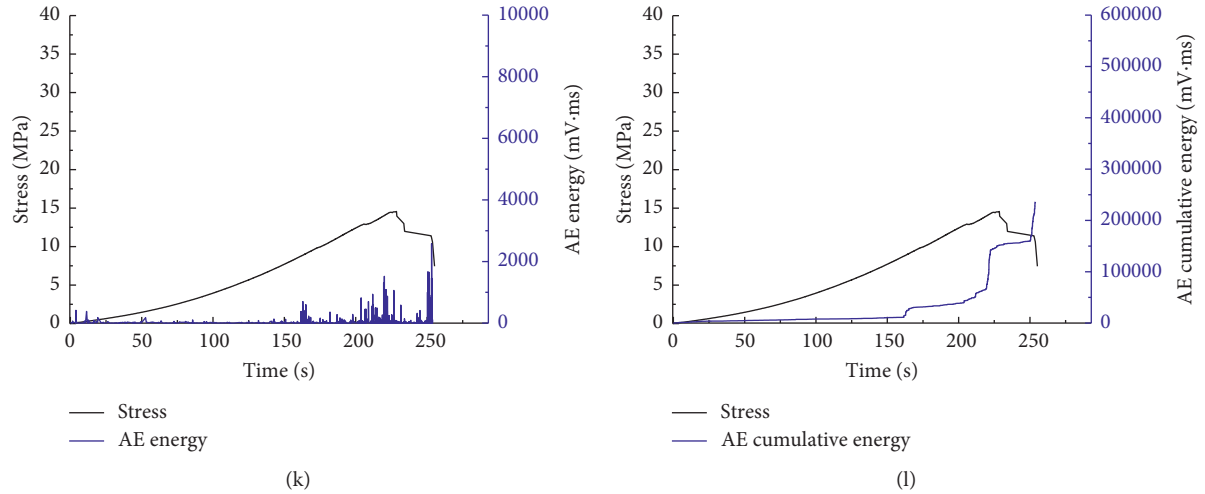

Figure 16: Relationship of AE signals and stress and time about coal samples of different gas pressures under uniaxial compression. (a, b, c, and d) Coal sample without gas: B1-2; (e, f, g, and h) Coal sample with 1 MPa gas pressure: B2-3; (i, j, k, and l) Coal sample with 2 MPa gas pressure: B3-2.

Table 7: AE signal of coal samples with different gas pressures under uniaxial loading.

Samples ID	Gas pressure (MPa)	AE peak energy (mV·ms)		AE cumulative energy (mV·ms)	
		Test value	Average value	Test value	Average value
B1-1	0	5896.6	6292.6	487103.5	473508.7
B1-2		8593.6		474759.9	
B1-3		4388.2		458662.8	
B2-1	1	2450.5	2950.7	380061.5	393460.7
B2-2		4066.6		398323.9	
B2-3		2335.2		401996.8	
B3-1	2	1860.2	2151.8	294909.8	275986.2
B3-2		2581.7		236050.5	
B3-3		2013.4		296998.3	

between the coal specimen and the environment during loading is assumed, and the relationship between the above energy is expressed as equations (7)–(9) [26]:

$$U = U_d + U_e, \tag{8}$$

$$U = \int_0^{\varepsilon} \sigma d\varepsilon, \tag{9}$$

$$U^e = \frac{\sigma^2}{2E_U}, \tag{10}$$

where U is the volumetric total input energy generated by external work, MJ/m^3; U^e is the volumetric elastic energy stored in the coal sample, MJ/m^3; U^d is the dissipated energy of the coal sample, MJ/m^3; E_U is the unloading modulus, which is assumed to be approximately equal to the loading elastic modulus for coal; and σ and ε are the stress and strain values of the coal sample during UCS test.

According to the above energy calculation formula and the relationship between them, the corresponding relationship between the each part energy evolution rule and the stress-strain curve of the coal sample in the process of loading under different gas pressures is obtained (due to the space limitation, this paper only lists some coal samples for description), as shown in Figure 17.

It can be seen from Figure 16 that the characteristics of energy changes during uniaxial compression of coal samples with different gas pressures have common features. In the initial compression phase, the coal sample is relatively complete, and the dissipative energy is mainly generated by the crack compression, in which the elastic energy and the dissipative energy are slowly increased. In the elastic phase, the coal body mainly produces elastic deformation, and the rate of increase of elastic energy is significantly accelerated, and the dissipation energy still slowly increases. When the coal sample reaches the peak stress, the elastic energy also reaches the peak value. In the postpeak phase, under the action of external force, the cracks in the coal sample begin to expand, penetrate, and block slip friction on a large scale, resulting in the formation of macrofracture surface and the loss of material strength, so the dissipative energy began to increase sharply. Due to the large-scale expansion of the cracks, the stability of the coal body decreases, and the elastic energy released in large quantities and began to show a downward trend. At the residual deformation phase, the energy is dissipated basically, and the external force is mainly used for friction and sliding between blocks.

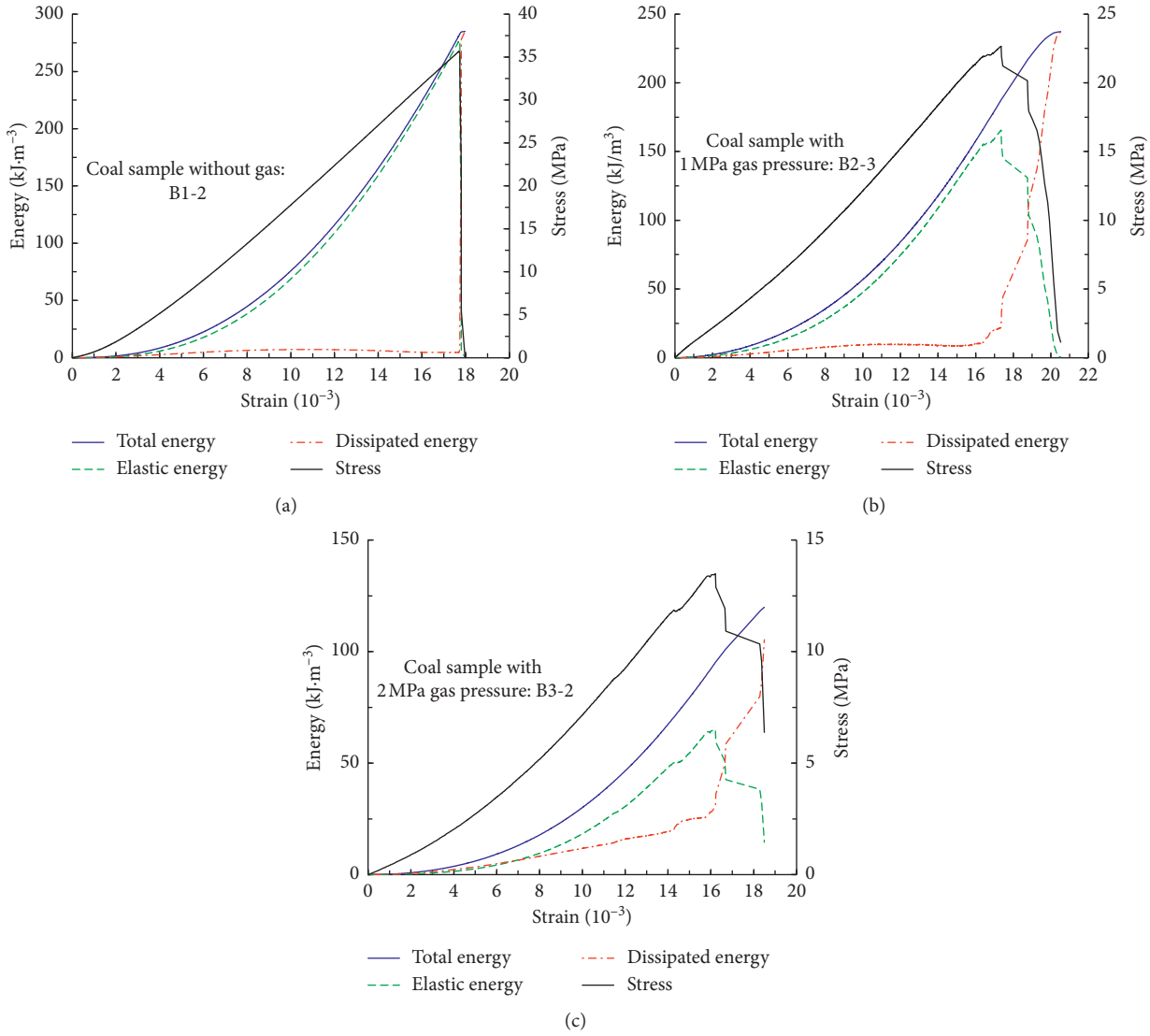

Figure 17: Energy evolution curve of coal samples of different gas pressures under uniaxial loading. (a) Coal sample without gas. (b) Coal sample with 1 MPa gas pressure. (c) Coal sample with 2 MPa gas pressure.

However, with the increase of gas pressure, the total energy, elastic energy, and dissipative energy in the process of coal sample loading decrease, and the characteristics of dissipative energy in the postpeak phase change obviously. The instantaneous release of elastic energy of gas-free coal samples at the postpeak phase is converted into dissipative energy, and the elastic energy of gas-free coal samples at postpeak phase instantaneously releases and converts into dissipative energy, which shows that the curve of dissipation energy rises almost vertically, reflecting the brittle failure of the coal sample in an instant, and the energy release is more intense during the failure. For gas-containing coal samples, the dissipative energy curve in the postpeak phase shows a gradual increase trend, indicating that the gas-containing coal samples do not undergo transient brittle failure and still have a certain bearing capacity, which reflects the failure characteristics of gas-containing coal samples which changed from brittle to ductile.

4. Discussion

4.1. Dilatancy Effect of Filling Gas and Adsorbing Gas on Coal Samples. It can be seen from the test results in Section 3.1 that the axial and lateral deformation (i.e., the volume of the coal sample) of the coal sample increase in the process of coal filling gas and adsorbing gas. Zhang believed that within a certain pressure range, the expansion deformation of the coal sample will increase with the increase of gas adsorption value, but the increase rate will gradually decrease, which is consistent with the results of this experiment [27].

In the gas filling progress, there is also a process of gas adsorption, but because the gas filling rate is much higher than the gas absorption rate of coal sample, it is considered that the deformation of the coal sample in the gas filling progress is mainly dominated by free-state gas, which acts on the skeleton and crack of the coal body in the form of volume force. Under the condition of lower gas pressure, the free-

state gas molecules can enter into the pore crack larger than the average free path of gas molecules. With the increase of gas pressure, the free-state gas molecules have the ability to open and enter the microcracks in the coal body, as shown in Figure 18, which causes tensile or shear failure of the coal body structure, thus forming the microfracture of the coal body [27, 28]. Under the action of free-state gas, the structure of the coal sample has changed, which promotes the expansion deformation of the coal sample.

With the gas adsorption to saturation, the gas pressure inside the coal body is gradually balanced with the gas pressure in the environment. The effect of adsorbed state gas on the coal sample is more obvious, which can reduce the surface free energy of coal matrix and the cementation force between coal particles. This will make it easier to produce microfracture by the action of expansion stress and thus expands the wedge-opening effect of free-state gas on coal pore and fissure [28, 29]. It can be found from Figure 6 that the lateral and axial strains of coal samples in the process of gas adsorption significantly increased, and the early strain rate of coal samples is relatively high, but the increase rate of strain decreases with the increase of adsorption time, and the greater the pressure, the greater the strain at adsorption saturation. In Figure 6, the deformation of the coal sample will fall back after reaching the peak value, which is caused by the fact that when the deformation peak is reached, the elastic stress generated by the coal sample is greater than the gas pressure, and the skeleton deformation of the coal body is partially restored. On the whole, the volume of the coal sample expands after gas adsorption.

Meanwhile, the NMR experiments of coal samples under different gas pressures were used to study the porosity characteristics of coal samples after gas adsorption. The test results are shown in Figure 19. The results show that the porosity of coal samples with saturated adsorption under 1 MPa and 2 MPa gas pressure is 1.869% and 2.771%, respectively. Compared with the coal sample without gas, the porosity increases by 20.1% and 78.1%, respectively, indicating that the internal porosity of coal samples increases after gas adsorption and the internal pore structure changes.

From what has been discussed above, the volume deformation of the original coal sample increases after filling and absorbing the gas. Due to the small volume change of the coal sample matrix, the expansion of the original coal sample is mainly caused by the increase of the internal pore and fracture structure, which makes the porosity of gas-containing coal increase and the integrity of gas-containing coal decrease compared with the original coal sample.

4.2. Analysis of Mechanical Properties of Gas-Containing Coal Samples. Figure 7 shows the relation curve of average UCS and average elastic modulus with gas pressure by the uniaxial compression test. It can be seen in this figure that the average UCS and the average elastic modulus of the coal sample decrease with the increase of the gas pressure. The above result shows that the participation of the gas changes the mechanical properties of the coal sample.

According to the previous research and the above discussion, it is believed that there are several reasons for the influence of gas on the mechanical properties of coal samples. Firstly, the participation of gas leads to the volume expansion of the coal sample, the increase of the internal pores and fissures, and the decrease of the integrity of the coal sample, which reduces the ability of the coal sample to resist damage and deformation under external loading. Secondly, after gas absorption, the surface energy of the hole and fissure inside the coal decreases and the distance between the coal particles increases. As the results, the cohesive force between coal particles decreases and the force needed to destroy coal structure reduces, so the ability of coal to bear deformation and failure is reduced. Thirdly, gas pressure increases the space between the holes and fissures in the coal body, which reduces the surface friction coefficient of those pores and fissures. Meanwhile, coal's internal gas compression will produce tensile stress at the tip of the hole crack when loading coal sample. The tensile strength of the coal sample is far smaller than the compressive strength, so the coal structure is more easily damaged.

Therefore, the mechanical response characteristics of coal samples are changed under the multiple actions of gas mechanics and nonmechanics, which generally shows that the strength of coal samples decreases with the increase of gas pressure.

4.3. Analysis of Energy Characteristics in the Process of Gas-Containing Coal Failure. Rock burst and coal and gas outburst are typical coal and gas dynamic disasters, and they happen because of the sudden release of elastic potential energy or internal energy of gas in coal and rock mass, which causes the sudden destruction of coal and rock medium. Similarly, the deformation and damage of coal samples from the microscopic perspective have experienced such stages as internal primary fracture compaction, new fracture generation, new fracture development, new fracture penetration, and macrofracture generation, which are also the result of the comprehensive action of energy accumulation, dissipation, and release. Energy dissipation is mainly used to induce rock mass damage, leading to the deterioration of coal-rock material properties and loss of strength, and energy release is the internal cause of rock mass sudden failure [26].

In this paper, several parameters, such as elastic strain energy index, impact energy index, AE energy index, and energy dissipation characteristic index, are used to research the energy characteristics of gas-containing coal in the process of loading and analyze the influence of gas on the burst characteristics in the process of coal sample damage. Elastic strain energy index and impact energy index are important indexes to evaluate the burst tendency of coal samples, which can reflect the macrocharacteristics of elastic energy accumulation and energy dissipation during the loading process of coal samples, and AE energy index and energy dissipation characteristic index can reflect the dynamic change rule of energy accumulation and dissipation with time in the process of loading gas-containing

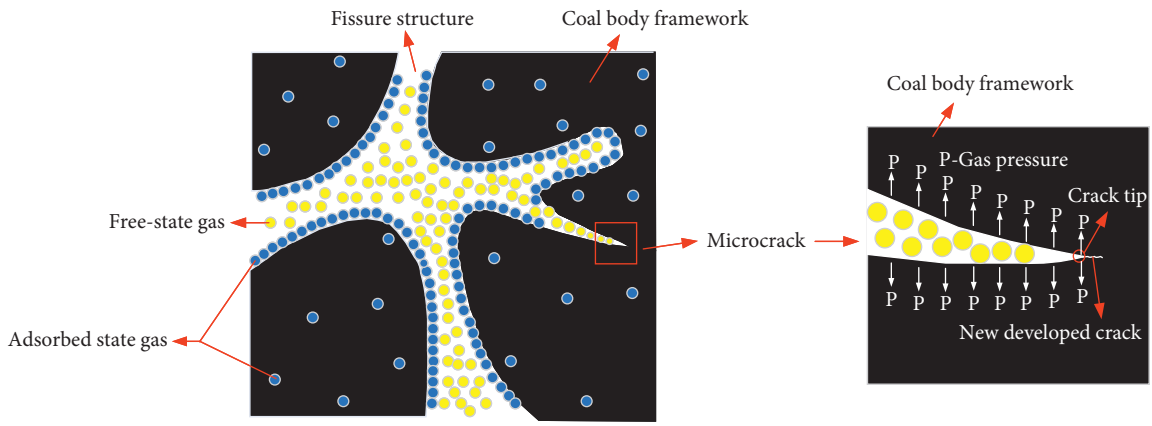

Figure 18: Wedge-opening effect of free gas on coal pore and fissure.

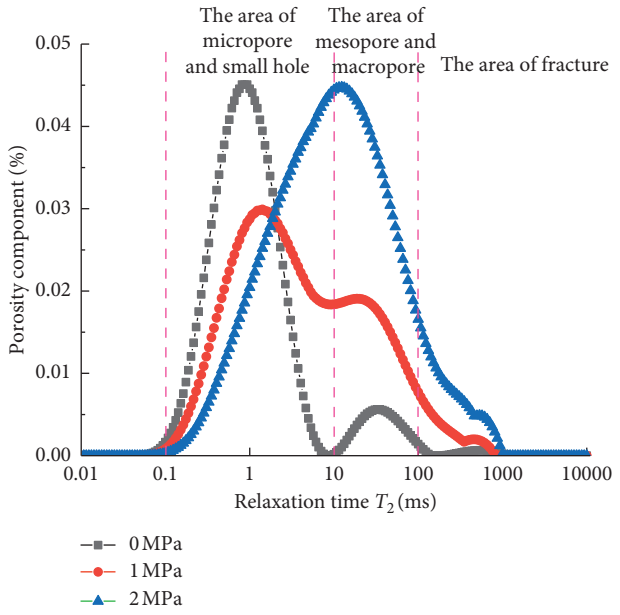

Figure 19: The T_2 distribution of the coal sample with different gas pressures.

coal. From the test data of elastic energy index and impact energy index of gas bearing coal in Sections 3.3 and 3.4, it can be seen that, with the increase of gas pressure, the elastic deformation of the coal sample decreases and the plastic deformation increases, and the accumulation of elastic energy decreases and the dissipation energy after the peak increases when the coal sample is under external load, reflecting that the failure form of the gas-containing coal samples change from brittleness to plasticity compared with the original coal sample, which shows that the participation of gas weakens the burst tendency of the coal sample. From the AE energy index and energy dissipation characteristic index in 3.5 and 3.6, it can be seen that compared with the coal samples without gas, the peak energy of the coal samples with gas decreases during the loading process, and the proportion of the accumulation of elastic energy decreases. In the postpeak stage, the energy release process of the gas-containing coal samples is gentler and the failure duration is long, showing that the ductile failure characteristics are relatively obvious.

The rules of the above four energy analysis indexes show that the participation of gas in the coal sample accelerates the dissipation of the elastic property before the coal sample is destroyed, which is not conducive to the released elastic property of the coal sample storage. Without considering the gas expansion energy, the existence of gas eases the destruction process of the coal sample and reduces the destruction energy of the rock burst, that is to say, compared with the original coal sample, the burst property of the gas bearing coal is reduced. The reasons for the above rules are as follows. First, in the process of gas filling and adsorption, the coal samples have the phenomenon of dilatancy. The porosity of the coal sample increases, which makes the microstructure of the coal samples more loose and easier to be broken, thus increasing the dissipative energy used for fracture damage and reducing the accumulated elastic energy of the coal sample. Second, when there is a certain gas pressure in the coal body, the load acting on the coal body is jointly borne by the gas pressure and the coal sample skeleton. Compared with the coal sample without gas, the effective stress of the coal sample with gas is reduced so that the accumulated elastic energy in the coal body is reduced. Last, the properties of the gas-containing coal sample changes due to the adsorption of gas in its inner surface, which reduces the tension of the inner pore surface of the coal body and the force between the coal particles. Thus, the strength of the coal body is weakened, and the u UCS and elastic modulus of the coal sample are reduced, which causes the energy accumulated before the destruction of the coal sample reduce.

Under the condition of deep mining, coal seam is faced with the joint action of high ground stress and high gas pressure, and the dynamic disaster of coal mine shows the characteristics of coal-rock gas composite dynamic disaster with rock burst and coal and gas outburst. In the deep mining environment, for the high gas coal seam with burst tendency, the existence of gas in the coal seam reduces the burst tendency of the coal sample to a certain extent because of the decrease of the integrity of the coal body and the

decrease of the strength of the coal body, causing the threshold value of dynamic disaster is reduced. Therefore, when evaluating the risk of dynamic disaster in deep gas-containing coal seam, the factors such as the nature of coal and rock mass, high ground stress, and high gas pressure should be comprehensively analyzed in order to formulate targeted prevention and control measures.

5. Conclusion

In this study, a novel gas-solid coupling loading apparatus is designed to realize gas adsorption of the coal sample with burst proneness and provide uniaxial loading environment under different gas pressures. A series of uniaxial compression tests of gas-containing coal with different gas pressures is carried out, and the energy dissipation process is monitored by an acoustic emission (AE) system. According to the experimental results, the conclusions are drawn as follows:

(1) Under the condition of constant uniaxial loading pressure, the macroscopic volume strain of the coal sample is proportional to the gas adsorption and gas pressure, indicating the gas can expand the pores and natural fractures in the coal sample by mechanical and physicochemical effects, which leads to a degradation in microstructure integrity of the coal sample.

(2) The dilatancy effect of gas on the coal sample changes the pore-fissure structure and the mesoscopic stress environment inside the coal sample, which changes the macroscopic mechanical properties of the coal sample. Both the macrouniaxial compression strength (UCS) and elastic modulus show a downward trend with the increase of gas pressure; the UCS and elastic modulus of coal samples with 2 MPa gas pressure reduce by 58.78% and 48.82%, respectively, compared to those of the original coal samples.

(3) Owing to the change of the mesostructure of gas-containing coal samples, the accumulated elastic energy of the gas-containing coal samples before failure reduces significantly, whereas the energy dissipated during loading increases, and the energy release process in the postpeak stage is smoother, indicating the participation of gas weakens the burst proneness of the coal sample. This study is of important scientific value for revealing the mechanism of combined dynamic disaster and the critical occurrence conditions of coal-rock burst and coal and gas outburst.

Data Availability

The data used to support the findings of this study are available from the corresponding author upon request.

Conflicts of Interest

The authors declare that the authors do not have conflicts of interest representing a conflict of interest in connection with the paper submitted.

Acknowledgments

The authors would like to express their gratitude to Professor Chengdong Su for his help in the experiment. The authors thank the State and Local Joint Engineering Laboratory for Gas Drainage and Ground Control of Deep Mines. This study was supported by the National Key R&D Program of China (2018YFC0604502), The Development Plan of Young Backbone Teachers in Colleges and Universities of Henan Province (2016GGJS-042), Joint Talent Fund of NSFC-The People's Government of Henan Province (U1304502), China Postdoctoral Science Foundation (2020M672227), and Natural Science Foundation of Henan Province (202300410175).

References

[1] R. F. Yuan, "Features of dynamic disasters combined rockburst and gas outburst in deep coal mine and its preventive measures," *Coal Science and Technology*, vol. 41, no. 8, pp. 6–10, 2013.

[2] Y. S. Pan, "Integrated study on compound dynamic disaster of coal-gas outburst and rockburst," *Journal of China Coal Society*, vol. 41, no. 1, pp. 105–112, 2016.

[3] P. G. Ranjith, J. Zhao, M. Ju, R. V. S. De Silva, T. D. Rathnaweera, and A. K. M. S. Bandara, "Opportunities and challenges in deep mining: a brief review," *Engineering*, vol. 3, no. 4, pp. 546–551, 2017.

[4] B. B. Gao, H. G. Li, H. M. Li et al., "Current situation of the study on acoustic emission and microseism monitoring of coupling dynamic catastrophe for gas-filled coal-rock," *Progress in Geophysics*, vol. 29, no. 2, pp. 0689–0697, 2014.

[5] M. T. Zhang, Z. H. Xu, Y. S. Pan et al., "A united insta-bilty theory on coal (rock) burst and outburst," *Journal of China Coal Society*, vol. 16, no. 4, pp. 48–53, 1991.

[6] T. Li, M. F. Cai, J. A. Wang et al., "Discussion on relativity between rockburst and gas in deep exploitation," *Journal of China Coal Society*, vol. 30, no. 5, pp. 562–567, 2005.

[7] Z. Wang, G. Z. Yin, Q. T. Hu et al., "Inducing and transforming conditions from rockburst to coal-gas outburst in a high gassy coal seam," *Journal of Mining & Safety Engineering*, vol. 27, no. 4, pp. 572–575, 2010.

[8] K. Wang and F. Du, "Coal-gas compound dynamic disasters in China: a review," *Process Safety and Environmental Protection*, vol. 133, pp. 1–17, 2020.

[9] R. F. Yuan, H. M. Li, and H. Z. Li, "Distribution of microseismic signal and discrimination of portentous information of pillar type rockburst," *Chinese Journal of Rock Mechanics and Engineering*, vol. 31, no. 1, pp. 80–85, 2012.

[10] H. B. Zhao, Z. H. Li, S. H. Zhong et al., "Experimental study of mechanical properties of coal rock containing gas under uniaxial compression," *Journal of Mining & Safety Engineering*, vol. 27, no. 1, pp. 131–134, 2010.

[11] A. K. Singh, R. Singh, J. Maiti, R. Kumar, and P. K. Mandal, "Assessment of mining induced stress development over coal pillars during depillaring," *International Journal of Rock Mechanics and Mining Sciences*, vol. 48, no. 5, pp. 805–818, 2011.

[12] S.-L. Wang, S.-P. Hao, Y. Chen, J.-B. Bai, X.-Y. Wang, and Y. Xu, "Numerical investigation of coal pillar failure under simultaneous static and dynamic loading," *International Journal of Rock Mechanics and Mining Sciences*, vol. 84, pp. 59–68, 2016.

[13] X. K. Qu, F. X. Jiang, H. T. Wang et al., "Research on mechanism of rock burst induced by coal pillar failure in mine

goaf," *Journal of Mining & Safety Engineering*, vol. 34, no. 6, pp. 1134–1140, 2017.

[14] J. Pan, Z. Zhang, M. Li, Y. Wu, and K. Wang, "Characteristics of multi-scale pore structure of coal and its influence on permeabilityfluence on permeability," *Natural Gas Industry B*, vol. 6, no. 4, pp. 357–365, 2019.

[15] J. W. Yan, Z. P. Meng, K. Zhang et al., "Pore distribution characteristics of various rank coals matrix and their influences on gas adsorption," *Journal of Petroleum Science and Engineering*, vol. 189, Article ID 107041, 2020.

[16] N. I. Aziz and M. L. W, "The effect of sorbed gas on the strength of coal - an experimental study," *Geotechnical and Geological Engineering*, vol. 17, no. 3, pp. 387–402, 1999.

[17] J. D. St. Ming-Li and M. A. Barakat, "The change in effective stress associated with shrinkage from gas desorption in coal," *International Journal of Coal Geology*, vol. 45, pp. 105–113, 2001.

[18] Z. Majewska, S. Majewski, and J. Ziętek, "Swelling and acoustic emission behaviour of unconfined and confined coal during sorption of CO_2 fined and confinedcoal during sorption of CO_2," *International Journal of Coal Geology*, vol. 116-117, pp. 17–25, 2013.

[19] G. Xie, Z. Yin, L. Wang, Z. Hu, and C. Zhu, "Effects of gas pressure on the failure characteristics of coal," *Rock Mechanics and Rock Engineering*, vol. 50, no. 7, pp. 1711–1723, 2017.

[20] L. D. Connell, "A new interpretation of the response of coal permeability to changes in pore pressure, stress and matrix shrinkage," *International Journal of Coal Geology*, vol. 162, pp. 169–182, 2016.

[21] W. He, W. G. Liang, B. N. Zhang et al., "Experimental study on swelling characteristics of CO2adsorption and storage in different coal rank," *Journal of China Coal Society*, vol. 43, no. 5, pp. 1408–1415, 2018.

[22] J. Chen, X. K. Pan, D. Y. Jiang et al., "Adsorption deformation characteristics of soft coal and hard coal to different gases under tri-axial stress condition," *Journal of China Coal Society*, vol. 43, no. S1, pp. 149–157, 2018.

[23] S. R. Zhai, "Experimental study on gas adsorption-desorption deformation characteristics of briquette coal samples with different granularity," *Journal of Safety Science and Technology*, vol. 14, no. 6, pp. 84–89, 2018.

[24] G. Z. Yin, Z. Wang, and D. M. Zhang, "Experiment of the gas effect on coal mechanical properties under zero effective confirming pressure," *Journal of Chongqing University*, vol. 33, no. 11, pp. 129–133, 2010.

[25] C. D. Su, X. X. Zhai, X. Z. Wei et al., "Influence of saturatuion period on bursting liability indices for coal seam 2# in qianqiu coal mine," *Chinese Journal of Rock Mechanics and Engineering*, vol. 33, no. 2, pp. 235–242, 2014.

[26] H. Xie, L. Li, R. Peng, and Y. Ju, "Energy analysis and criteria for structural failure of rocks," *Journal of Rock Mechanics and Geotechnical Engineering*, vol. 1, no. 1, pp. 11–20, 2009.

[27] Z. G. Zhang, Q. J. Qi, S. G. Cao et al., "Characteristics of coal deformation during its adsorption of He, CH4 and CO2," *Journal of China Coal Society*, vol. 43, no. 9, pp. 2484–2490, 2018.

[28] X. Q. He, E. Y. Wang, and H. Y. Lin, "Coal deformation and fracture mechanism under pore gas action," *Journal of China University of Mining & Technology*, vol. 25, no. 1, pp. 6–11, 1996.

[29] G. Wang, Y. Guo, C. A. Du et al., "Experimental study on damage and gas migration characteristics of gas-bearing coal with different pore structures under sorption-sudden unloading of methane," *Geofluids*, vol. 2019, Article ID 7287438, 11 pages, 2019.